H-6-02 Extended Abstracts of the 2020 International Conference on Solid State Devices and Materials, VIRTUAL conference, 2020, pp545-546

Mid-infrared photoresponse due to cyclotron resonance absorption in graphene/h-BN van der Waals heterostructures

Tomoki Machida[1], Momoko Onodera[1], Satoru Masubuchi[1], Kei Kinoshita[1], Rai Moriya[1], Kenji Watanabe[2], and Takashi Taniguchi[3,1]

[1] Institute of Industrial Science, Univ. of Tokyo
4-6-1, Komaba, Meguro-ku, Tokyo 153-8505, Japan
Phone: +81-3-5452-6742 E-mail:tmachida@iis.u-tokyo.ac.jp
[2] Research Center for Functional Materials, National Institute for Materials Science
1-1 Namiki, Tsukuba 305-0044, Japan
[3] International Center for Materials Nanoarchitectonics, National Institute for Materials Science
1-1 Namiki, Tsukuba 305-0044, Japan

Abstract

Charge carriers in graphene, massless Dirac fermions, form a unique sequence of the Landau levels in high magnetic fields. Thus, the cyclotron resonance (CR) in graphene is distinctly different form that in conventional two-dimensional electron systems based on semiconductors. In this work, we study mid-infrared/THz photoresponse due to CR in graphene/h-BN van der Waals heterostructures. In particular, we focus on CR in a dual-gated trilayer graphene/h-BN [1] and a monolayer graphene under double-moiré potentials [2].

1. CR in dual-gated trilayer graphene

ABA-stacked trilayer graphene (TLG) possesses both monolayer graphene (MLG)-like and bilayer graphene (BLG)-like bands. In a high perpendicular magnetic field B, the energy interval of Landau levels (LLs) in TLG is in a wavelength range from mid-infrared to near-infrared, which is technologically important for optoelectronics application. By applying a perpendicular electric displacement field D, a band gap is induced, and D hybridizes MLG-like and BLG-like bands in TLG, which appears as anti-crossings of LLs. Thus, ABA-stacked TLG has an electrical tunability of LLs in a large extent, which enables electrical tuning of cyclotron resonance (CR) magnetic field in TLG.

To demonstrate the electrical tunability of CR signals in TLG, we fabricate a dual-gated TLG device in which we can control D by applying bias voltage to the top and bottom gate electrodes. Figs. 1a-c show the schematic illustrations and optical image of TLG device in the present work. After exfoliation of h-BN flakes onto a 290-nm-thick SiO_2/p-doped Si substrate, TLG was transferred onto h-BN using a method based on polypropylene carbonate (PPC) [3,4]. Before capping it with another h-BN flake, we put electrodes on TLG by metal deposition of Pd 15 nm. Then the top h-BN layer was transferred onto the stack and a graphite (6~8 layers) was put on the top of it as a transparent top gate. Figs. 1d-g show color maps of the photo-induced voltage V_{photo} at the charge neutrality point $\nu = 0$ irradiated by laser light of different wavelengths of λ = 9.250, 9.552, 10.247, and 10.611 μm, respectively, as a function of D and B. We set the Fermi energy at the charge neutrality point by sweeping V_{BG} and V_{SD} along the line of R_{xx} peak in V_{SD}-V_{BG} plot. In these maps, the peak position of V_{photo} depends on D, drawing a curve which is symmetric to $D = 0$. These curves of V_{photo} evidently shows that CR signals in TLG is distinctly modified by D.

To give an account for D dependence of CR signals, we calculated LL diagram by tight-binding approximation with different Δ_1 ranging from 0 to 40 meV, where Δ_1 is proportional to D. Using the calculated LLs, we obtained a position of B for each Δ_1 where the LL interval is equal to the energy of irradiated laser, where CR transition between LLs is allowed. The numerical plot reproduces the experimental results quite well. These agreement of calculation and experiment demonstrate that LLs in TLG is successfully tuned in our dual-gated TLG device. At the same time, CR signals directly reflects the energy interval of LLs, thus it can be utilized as a powerful probe to study LLs in TLG quantum Hall systems.

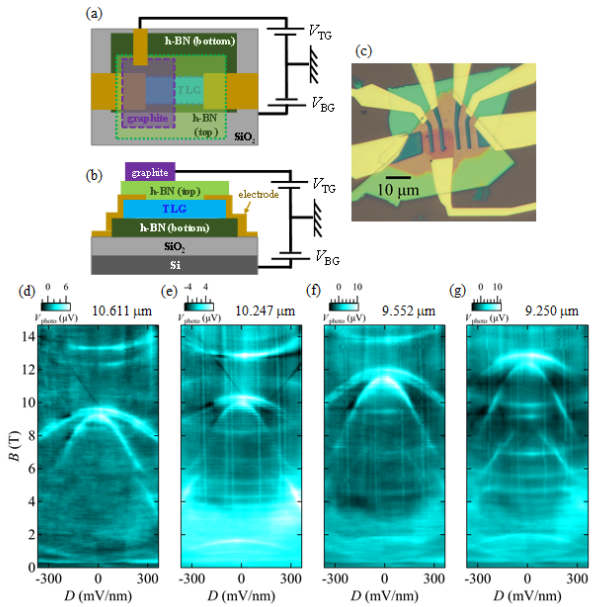

Fig. 1 (a) Top- and (b) side-view schematics of the device structure. (c) Optical image of the device. (d-g) Color map of V_{photo} as a function of D and B at $\nu = 0$ (experiment).

2. CR in graphene under double-moiré potentials

When the crystal axis of graphene is aligned to that of adjacent hexagonal boron nitride (h-BN), graphene's band structure is modified by the moiré potentials induced at the interface, exhibiting unique physical phenomena such as Hofstadter butterfly. Recently, it was found that two coexisting moiré potentials in a h-BN/graphene/h-BN heterostructure interfere with each other to generate second-order moiré potentials. Here, we study cyclotron resonance (CR) in graphene in double-moiré potentials, which provide us a direct insight on Landau levels (LLs) in graphene.

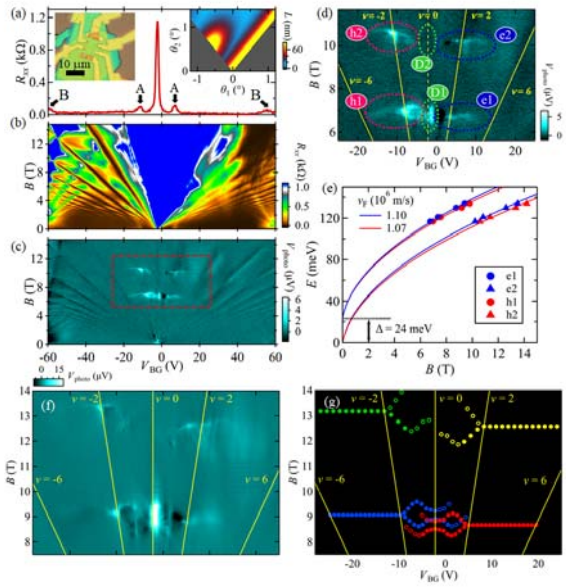

Fig. 2 (a) R_{xx} vs V_{BG} at $T = 3$ K and $B = 0$. Left inset: photograph of the device. Right inset: second-order moiré wavelength as a function of θ_1 and θ_2. (b) R_{xx} vs V_{BG} and B at $T = 3$ K. (c) V_{photo} intensity vs V_{BG} and B with a light wavelength of $\lambda = 10.611$ μm. (d) Expanded view of the region in (c) indicated by the dashed-red outline. (e) Fitting to the experiment. (f) Experimental V_{photo} map as a function of V_{BG} and B with a light wavelength $\lambda = 9.536$μm. Yellow lines indicate the locations of $\nu = 0, \pm2, \pm6$. (g) Calculated B_{CR} corresponding to the experimental CR map shown in (f).

We fabricated a h-BN/graphene/h-BN heterostructure by layer-by-layer assembly using a method based on polypropylene carbonate (PPC). R_{xx}-V_{BG} plot and Landau fan at $T = 1.6$ K show satellite peaks very close to the Dirac point, which is an indicative of a moiré potential with a large period [Figs. 2a,b]. From the position of these R_{xx} peaks, we estimated the lateral orientation angle θ between graphene and two h-BN sheets as θ~0.73° and ~1.01°. Next, we measured photo-induced voltage V_{photo} under the irradiation of mid-infrared light at $T = 3$ K. By sweeping carrier density, we observed unique patterns of CR signals, which are distinct from those in conventional graphene without moiré potentials [Fig. 2c]. To account for the distinct signal patterns, we consider electron-hole asymmetry in the Fermi velocity v_F and a large bandgap Δ induced at the Dirac point [Figs. 2d,e]. Based on this model, we fitted the CR magnetic field B_{CR} of these signals and derived $v_F = 1.10\times10^6$ m/s for electrons, $v_F = 1.07\times10^6$ m/s for holes, and $\Delta = 24$ meV [Fig. 2f]. We could precisely determine Δ and v_F because B_{CR} is highly sensitive to v_F and that we could observe inter-band and intra-band LL transitions by sweeping carrier density. Besides, CR signals have a unique ring-like shape, which we attributed to the enhancement of spin splitting owing to many-body interaction [Fig. 2g]. Our work will aid in understanding the band structure of double-moiré graphene and also demonstrate that CR is a powerful tool to reveal the LL structures.

Acknowledgements

This work was supported by CREST, Japan Science and Technology Agency (JST) under grant number JPMJCR15F3.

References

[1] M. Onodera, T. Taniguchi, K. Watanabe, M. Isayama, S. Masubuchi, R. Moriya, and T. Machida, Nano Letters **19**, 7282 (2019).

[2] M. Onodera, K. Watanabe, M. Isayama, M. Arai, S. Masubuchi, R. Moriya, T. Taniguchi, and T. Machida, Nano Letters **20**, 735 (2019).

[3] K. Kinoshita, R. Moriya, M. Onodera, Y. Wakafuji, S. Masubuchi, K. Watanabe, T. Taniguchi, and T. Machida, npj 2D Materials and Applications **3**, 22 (2019).

[4] M. Onodera, S. Masubuchi, R. Moriya, and T. Machida, Jpn. J. Appl. Phys. **59**, 010101 (2020)

[5] K. Kinoshita, R. Moriya, M. Arai, S. Masubuchi, K. Watanabe, T. Taniguchi, and T. Machida, Appl. Phys. Lett. **113**, 103102 (2018).

[6] K. Kinoshita, R. Moriya, S. Masubuchi, K. Watanabe, T. Taniguchi, and T. Machida, Appl. Phys. Lett. **115**, 153102 (2019).

[7] Y. Wakafuji, R. Moriya, S. Park, K. Kinoshita, S. Masubuchi, K. Watanabe, T. Taniguchi, and T. Machida, Appl. Phys. Lett. **115**, 143101 (2019).

[8] M. Onodera, K. Kinoshita, R. Moriya, S. Masubuchi, K. Watanabe, T. Taniguchi, and T. Machida, Sensors & Materials **31**, 2281 (2019).